Coexistence phenomena in neutron-rich A~100 nuclei within beyond-mean-field approach

A. PETROVICI

Horia Hulubei National Institute for Physics and Nuclear Engineering, Bucharest, Romania

Outline

- ***complex* EXCITED VAMPIR** *beyond-mean-field model*

- ***neutron-rich A~100 nuclei***

    - ***triple shape coexistence and shape evolution in the N=58 Sr and Zr isotopes***

    - ***shape evolution in even-even Zr nuclei***

    - ***Gamow-Teller β-decay relevant for :***

        - ***r-process (^{104,106}Zr)***

        - ***reactor decay heat (^{102,104}Tc)***

Characteristic features of neutron-rich A~100 nuclei

- *shape transition, shape coexistence, shape mixing*
- *drastic changes in structure with particle number, spin, excitation energy*

Open problems for theoretical models

- *realistic effective Hamiltonians and adequate large model spaces*
- *beyond-mean-field models*

Goals

- *unitary description of evolution in structure at low and high spins*
- *unitary treatment of structure and β-decay properties*

complex VAMPIR model family

- **the model space is defined by a finite dimensional set of spherical single particle states**

- **the effective many-body Hamiltonian is represented as a sum of one- and two-body terms**

- **the basic building blocks are Hartree-Fock-Bogoliubov (HFB) vacua**

- **the HFB transformations are essentially *complex* and allow for proton-neutron, parity and angular momentum mixing being restricted by time-reversal and axial symmetry**

- **the broken symmetries (s=N, Z, I, p) are restored by projection before variation**

∗ The models allow to use rather large model spaces and realistic effective interactions

Beyond-mean-field variational procedure: complex EXCITED VAMPIR model

Vampir

$$E^s[F_1^s] = \frac{\langle F_1^s|\hat{H}\hat{\Theta}^s_{00}|F_1^s\rangle}{\langle F_1^s|\hat{\Theta}^s_{00}|F_1^s\rangle}$$

Θ^s_{00} - symmetry projector

$|F^s_1>$ - HFB vacuum

$$|\psi(F_1^s); sM\rangle = \frac{\Theta^s_{M0}|F_1^s\rangle}{\sqrt{\langle F_1^s|\hat{\Theta}^s_{00}|F_1^s\rangle}}$$

Excited Vampir

$$|\psi(F_i^s); sM\rangle = \Sigma^i_{j=1}|\phi(F_j^s)\rangle\,\alpha^i_j \qquad \text{for} \quad i = 1, ..., n-1$$

$$|\phi(F_i^s); sM\rangle = \hat{\Theta}^s_{M0}|F_i^s\rangle$$

$$|\psi(F_n^s); sM\rangle = \Sigma^{n-1}_{j=1}|\phi(F_j^s)\rangle\,\alpha^n_j + |\phi(F_n^s)\rangle\,\alpha^n_n$$

$$(H - E^{(n)}N)f^n = 0$$

$$(f^{(n)})^+ N f^{(n)} = 1$$

$$|\Psi^{(n)}_\alpha; sM> = \sum_{i=1}^{n}|\psi_i; sM>f^{(n)}_{i\alpha}, \qquad \alpha = 1, \ldots, n$$

A~100 mass region

^{40}Ca - core

model space for both protons and neutrons :

$1p_{1/2}$ $1p_{3/2}$ $0f_{5/2}$ $0f_{7/2}$ $2s_{1/2}$ $1d_{3/2}$ $1d_{5/2}$ $0g_{7/2}$ $0g_{9/2}$ $0h_{11/2}$

(single-particle energies adjusted within complex MONSTER (VAMPIR))

renormalized G-matrix (OBEP, Bonn A)

- ***pairing properties enhanced by short range Gaussians for:***

  T = 1 pp, np, nn channels

  T = 0, S = 0 and S = 1 channels

- ***onset of deformation influenced by monopole shifts:***

  $<0g_{9/2}\ 0f;\ T=0\ |G|\ 0g_{9/2}\ 0f; T=0>$

- ***Coulomb interaction between valence protons added***

Triple shape coexistence and shape evolution in the N=58 Sr and Zr isotopes

A. Petrovici, Phys. Rev. C85 (2012) 034337

Neutron-rich Sr and Zr isotopes: - *rapid transition from spherical to deformed shapes*
- *sudden onset of quadrupole deformation for N > 58*

Positive parity states up to spin 20$^+$ in ^{96}Sr and ^{98}Zr (12-dimensional *EXVAM many-nucleon bases*)

The amount of mixing for the lowest 0^+ states of ^{96}Sr.

$I[\hbar]$	spherical	prolate	oblate
0_1^+	36%	20%	44%
0_2^+	57%	18%	25%
0_3^+		69%	31%
0_4^+	4%	6%	90%

Particular case for 0$^+$ states

· the lowest 0^+ VAMPIR configuration is spherical

· the 3-lowest 0^+ orthogonal EXVAM configurations (*s, o, p*) are situated in an energy interval of 375 keV

· maximum oblate-prolate mixing for 2^+ and 4^+ states

$\Delta E\ (2^+_{oblate} - 2^+_{prolate}) = 24$ keV

$\Delta E\ (4^+_{prolate} - 4^+_{oblate}) = 154$ keV

· spherical EXVAM configurations for spins 2^+ and 4^+ not found up to 4 MeV excitation energy

The mixing for the 2^+ and 4^+ states.

$I[\hbar]$	prolate	oblate
2_1^+	34(2)%	58(5)%
2_2^+	65%	33(2)%
4_1^+	56(1)%	36(6)%
4_2^+	43%	52(5)%

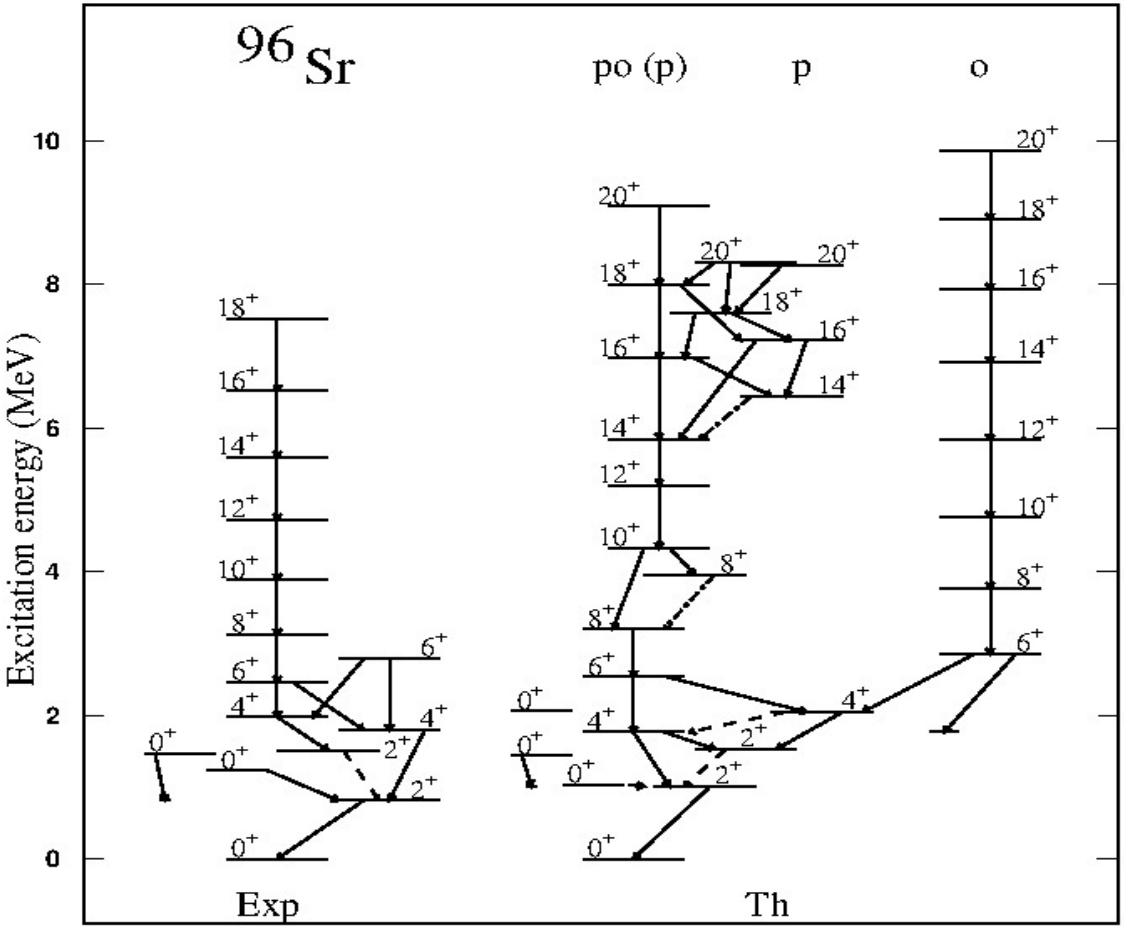

po(p)-band *- strong prolate-oblate mixing at low spins*

- variable prolate mixing at higher spins

almost pure o-band *feeds the second* 4^+ *(maximum o-p mixing)*

- the 3-lowest 0^+ EXVAM configurations (s, p, o) are separated by 323 keV

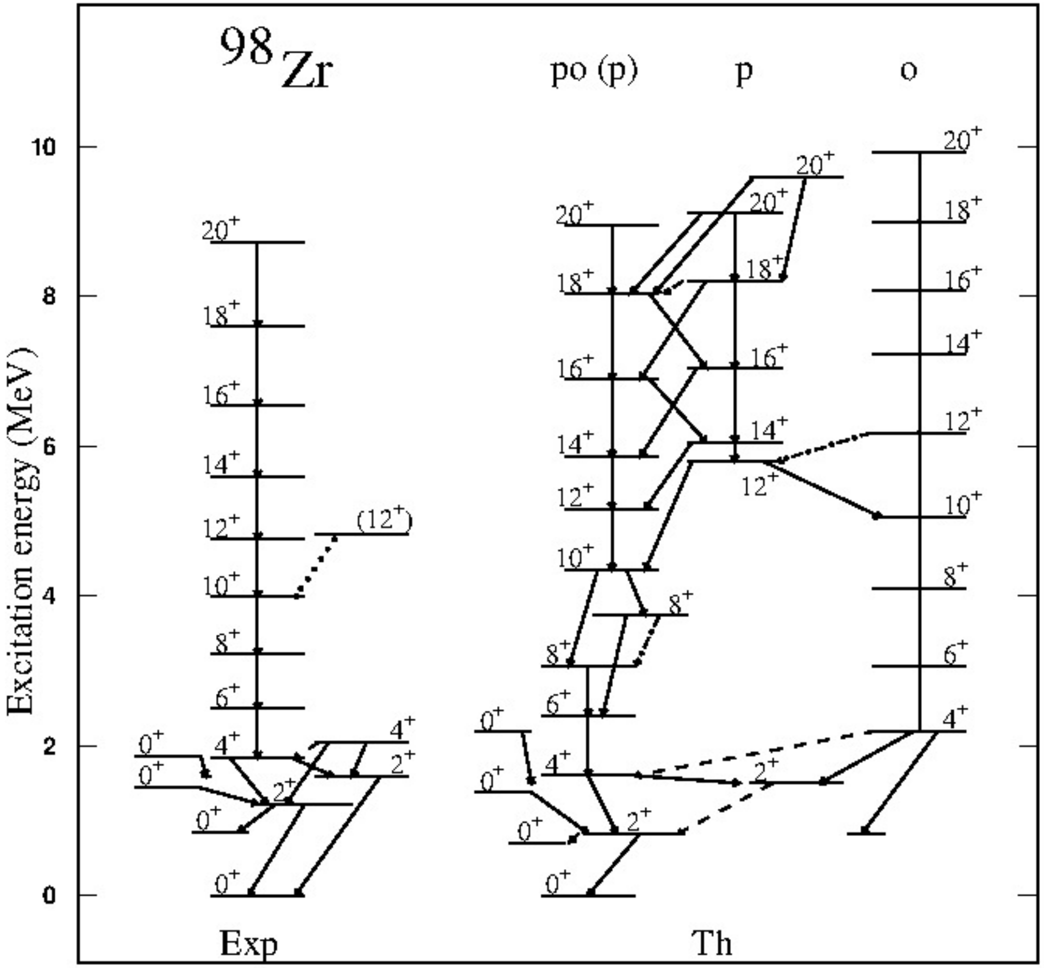

The amount of mixing for the lowest 0^+ states of ^{98}Zr.

$I[\hbar]$	spherical	prolate	oblate
0_1^+	12%	43%	45%
0_2^+	84%	12%	4%
0_3^+	1%	57%	42%
0_4^+	2%	10%	88%

- strong prolate-oblate mixing

$\Delta E\ (2^+_{prolate} - 2^+_{oblate}) = 206$ keV

$\Delta E\ (4^+_{prolate} - 4^+_{oblate}) = 431$ keV

The mixing for the 2^+ and 4^+ states.

$I[\hbar]$	prolate	oblate
2_1^+	60(8)%	31%
2_2^+	36%	63(1)%
4_1^+	83(7)%	10%
4_2^+	13(1)%	85(1)%

po(p)-band *- strong prolate-oblate mixing at low spins*

- variable prolate mixing at higher spins

o-band *feeds the second 2^+ (maximum o-p mixing)*

- spherical EXVAM configurations for spins 2^+ and 4^+ not found up to 4 MeV excitation energy

Occupation of valence single-particle orbitals for 0^+ states – sensitive to intrinsic deformation

$d^{\nu}_{5/2}$ occupation – essential for spherical 0^+ EXVAM configuration

$g^{\pi}_{9/2}$ occupation – significantly changing from intrinsically oblate to prolate deformed 0^+ EXVAM configurations

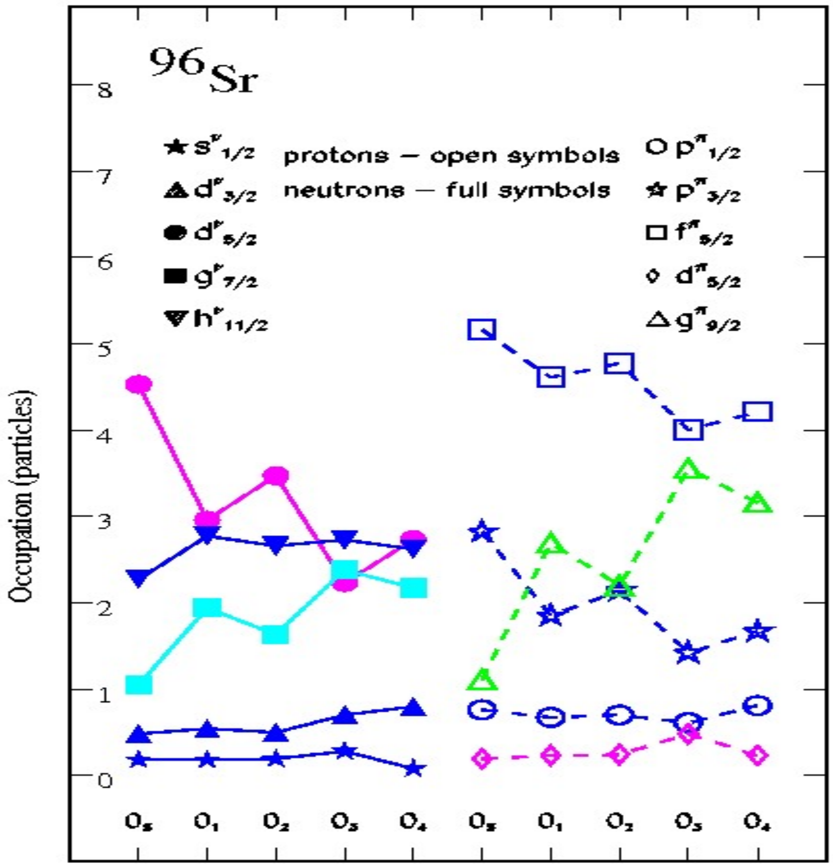

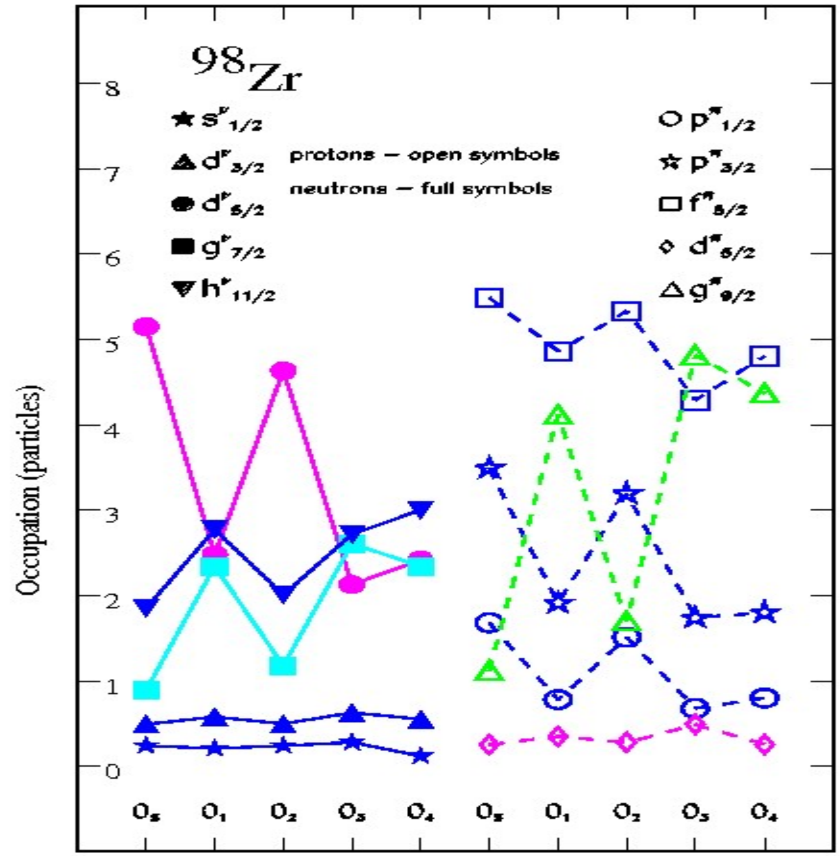

Strong E0 transitions support mixing of differently deformed configurations in 0^+ wave functions

$\rho^{2\,exp}_{max}(E0;0^+_3 \rightarrow 0^+_2) = 0.180$

$\rho^{2\,EXVAM}_{max}(E0;0^+_2 \rightarrow 0^+_1) = 0.066$

$\rho^{2exp}_{max}(E0;0^+_3 \rightarrow 0^+_2) = 0.075(8)$

$\rho^{2\,EXVAM}_{max}(E0;0^+_2 \rightarrow 0^+_1) = 0.060$

Evolution in structure with spin and excitation energy revealed by relevant spherical occupations

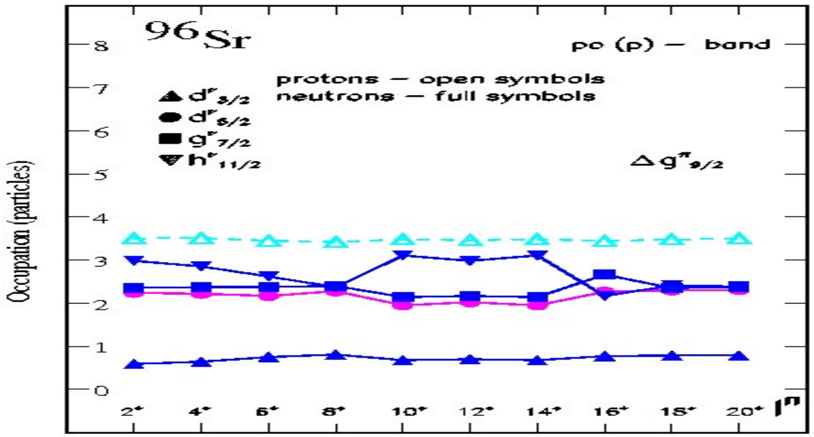

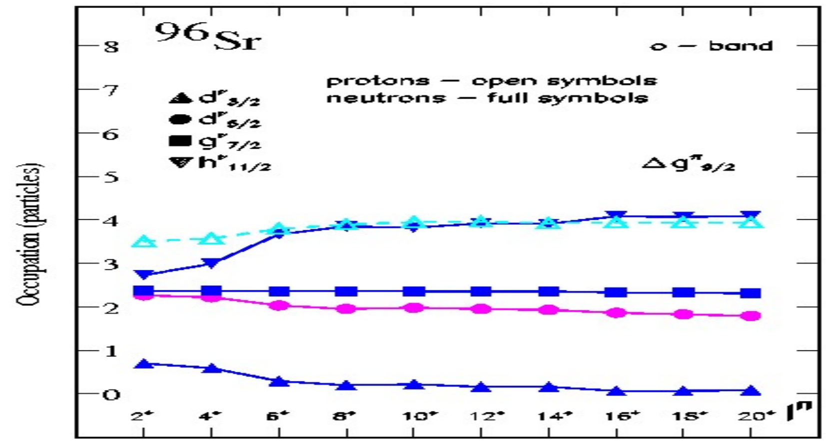

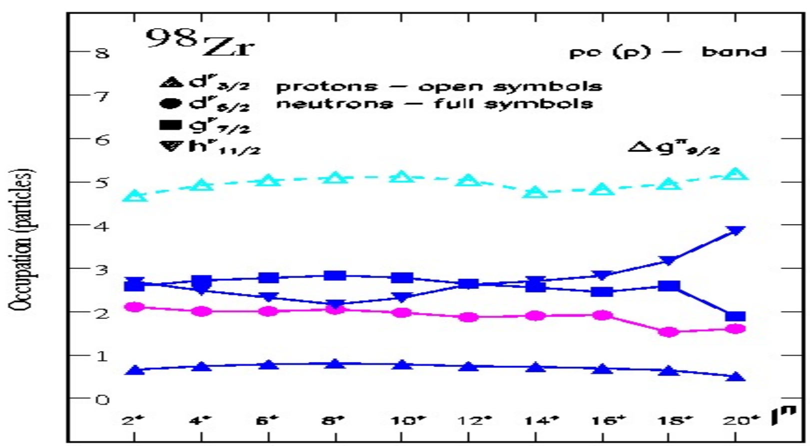

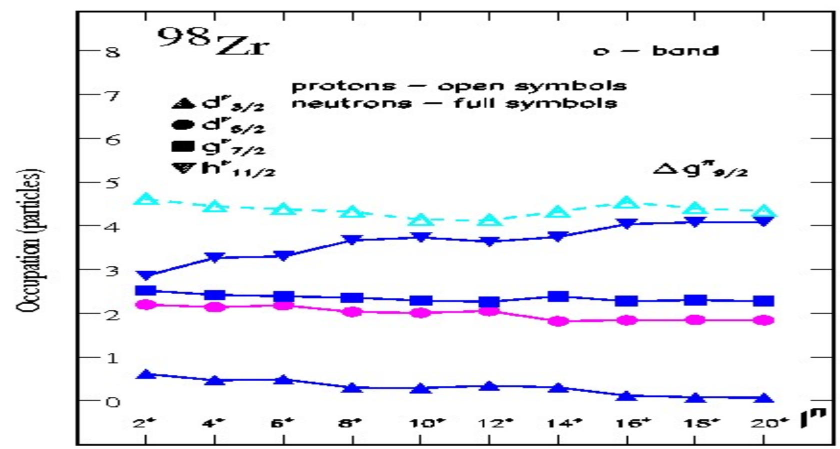

changes in structure corroborated with underlying shapes and evolution of shape mixing

Changes in structure revealed by angular momentum alignment and magnetic properties

dominant contribution from ν-$h_{11/2}$ and π-$g_{9/2}$ alignment

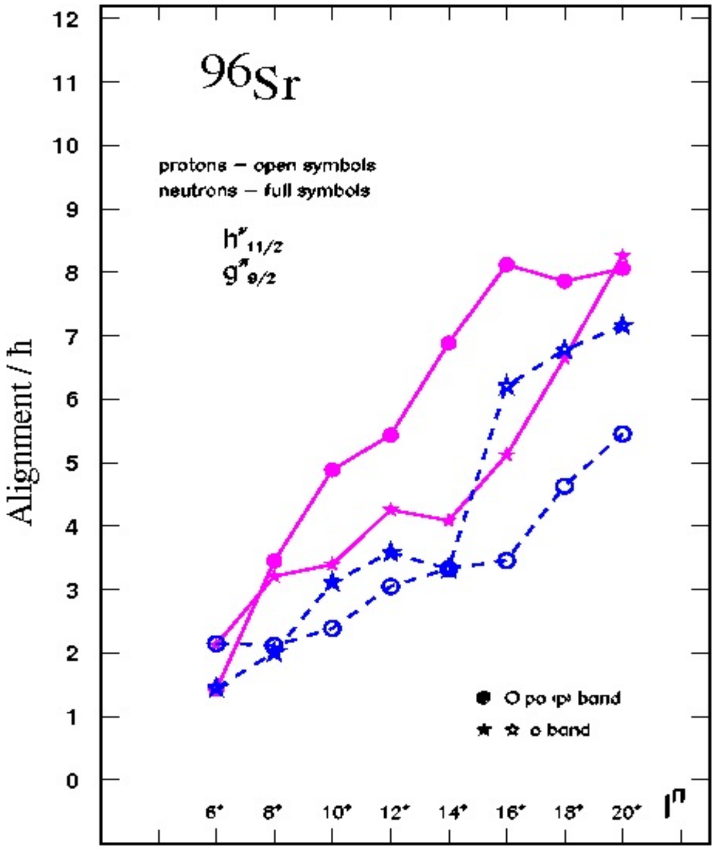

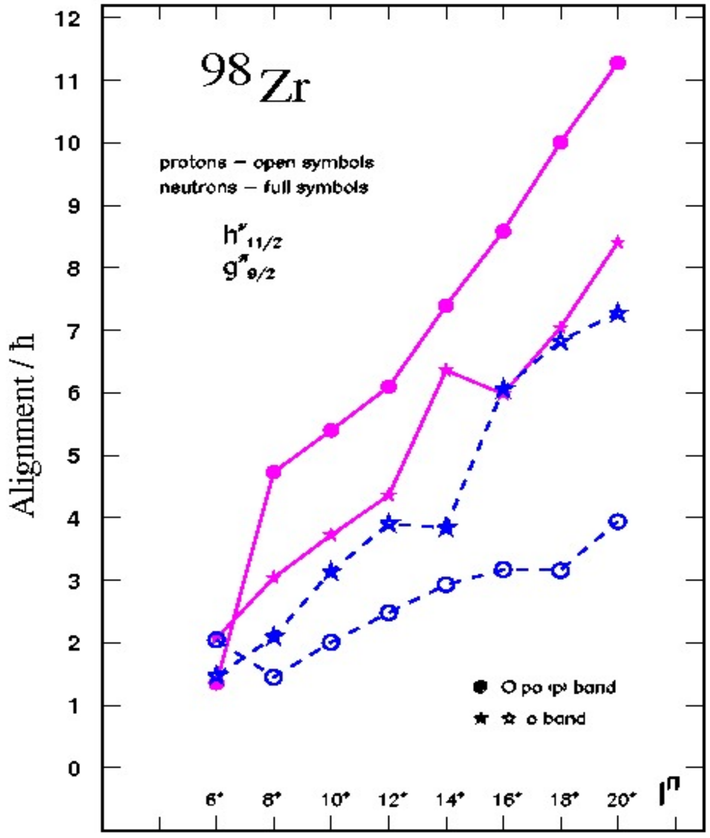

• *g-factor :* ≅ 0.24 ($I^{\pi} \geq 8^{+}$) (po(p)-band)
* *g-factor :* ≅ 0.50 ($I^{\pi} \geq 10^{+}$) (o-band)

• *g-factor :* ≅ 0.14 ($I^{\pi} \geq 8^{+}$) (po(p)-band)
* *g-factor :* ≅ 0.44 ($I^{\pi} \geq 10^{+}$) (o-band)

$B(M1;\, 8^{+}_{3} \rightarrow 8^{+}_{1}) = 1.29\ \mu^{2}_{N}$

$B(M1;\, 8^{+}_{2} \rightarrow 8^{+}_{1}) = 1.60\ \mu^{2}_{N}$

B(E2;ΔI = 2) strengths → fragmentation ↔ mixing

$B(E2; I \rightarrow I-2)$ values (in e^2fm^4) for the lowest bands of ^{96}Sr (EXVAM) (effective charges $e_p = 1.3$, $e_n = 0.3$).

$I[\hbar]$	$po(p)$-band	o-band
2^+	795 ***340(209) (old)*** ***580 (preliminary-Isolde)***	
4^+	1770 (187)	1901 (12)
6^+	1911 (560)	1484 (215) (89)
8^+	2127 (361)(122)	1436 (159) (121) (99)
10^+	819 (1329) (168)	1514 (231)
12^+	2332 (142)	1760
14^+	2354 (57) (44)	1392
16^+	238 (2237) (160)	1590
18^+	753 (1374) (248)	1459
20^+	2183 (97)	1359

$B(E2; I \rightarrow I-2)$ values (in e^2fm^4) for the lowest bands of ^{98}Zr (EXVAM) (effective charges $e_p = 1.3$, $e_n = 0.3$) .

$I[\hbar]$	$po(p)$-band	p-band	o-band
2^+	1140 (198)(161)		1305 (28) (18) (15)
4^+	2072 (620)		1593 (56)
6^+	2558 (101)		1662
8^+	1802 (942)(153)		1572 (123)
10^+	719 (1430)		1314 (119) (100)
12^+	2300 (216)	731 (345) (212)	663 (621) (307)
14^+	2428 (123)	1840 (392)	1094 (494)
16^+	1360 (832) (190)	548 (246) (1421)	602 (250) (195)
18^+	863 (207) (1416)	1347 (713) (808)	1115
20^+	409 (1958)	347 (185) (1972)	1313

Experimental lifetimes for intermediate spin states: simultaneous fit to several levels suggests deformation

$Q^{exp}_0\ (12^+ \rightarrow 10^+ \rightarrow 8^+) = 220\ (15)\ efm^2$

$Q^{exp}_0\ (12^+ \rightarrow 10^+ \rightarrow 8^+ \rightarrow 6^+) = 200\ (10)\ efm^2$

Spectroscopic quadrupole moments → deformation and mixing

Q_2^{sp} (in efm^2) for the lowest bands of ^{96}Sr (effective charges $e_p = 1.3$, $e_n = 0.3$).

$I[\hbar]$	po(p)	o
2^+	9.5	***0 (preliminary-Isolde)***
4^+	-23.9	1.4
6^+	-100.3	75.5
8^+	-120.1	77.3
10^+	-120.7	94.4
12^+	-124.1	94.6
14^+	-124.5	90.5
16^+	-130.0	85.4
18^+	-126.2	80.1
20^+	-124.4	68.1

Q_2^{sp} (in efm^2) for the lowest bands of ^{98}Zr (effective charges $e_p = 1.3$, $e_n = 0.3$).

$I[\hbar]$	po(p)	p	o
2^+	-36.6		7.1
4^+	-89.6		54.7
6^+	-115.5		76.7
8^+	-126.7		70.7
10^+	-130.1		58.2
12^+	-129.1	-98.5	55.6
14^+	-126.1	-121.2	30.5
16^+	-126.6	-123.0	60.8
18^+	-124.2	-134.4	74.9
20^+	-125.6	-135.4	68.9

po(p)-band: $\beta_2^{EXVAM}(8^+/10^+/12^+) \cong 0.3$

o-band: $\beta_2^{EXVAM}(8^+/10^+/12^+) \cong -0.19 \div -0.23$

o-band: $\beta_2^{EXVAM}(8^+/10^+/12^+) \cong -0.17 \div -0.13$

Gamow-Teller β decay of ^{102}Tc and ^{104}Tc (reactor decay heat)

M.D. Jordan, A. Algora A. Petrovici et al., Phys. Rev. C87 (2013) 044318

$^{102}Tc_{59} \rightarrow {}^{102}Ru_{58}$

$Q_{\beta} = 4.532 \pm 0.009$ MeV

$1^{+}_{gs} \rightarrow 0^{+}$ / 1^{+} / 2^{+}

$T_{1/2} = 5.28(15)$ s

$^{104}Tc_{61} \rightarrow {}^{104}Ru_{60}$

$Q_{\beta} = 5.516 \pm 0.006$ MeV

$3^{+}_{gs} \rightarrow 2^{+}$ / 3^{+} / 4^{+}

$T_{1/2} = 1098(18)$ s

complex EXCITED VAMPIR wave functions

$1^{+}_{gs} \rightarrow$ 53% oblate / 47% prolate
(7 EXVAM components)

$3^{+}_{gs} \rightarrow$ > 99% prolate
(7 EXVAM components)

$^{102}Ru_{58}$

complex EXCITED VAMPIR bases:

26 orthogonal projected configurations

for the spins 0^+, 1^+, 2^+

Gamow-Teller contributing states

0^+ : from 85% to 26% prolate components including almost spherical ones

2^+ : from 78% to 26% prolate components

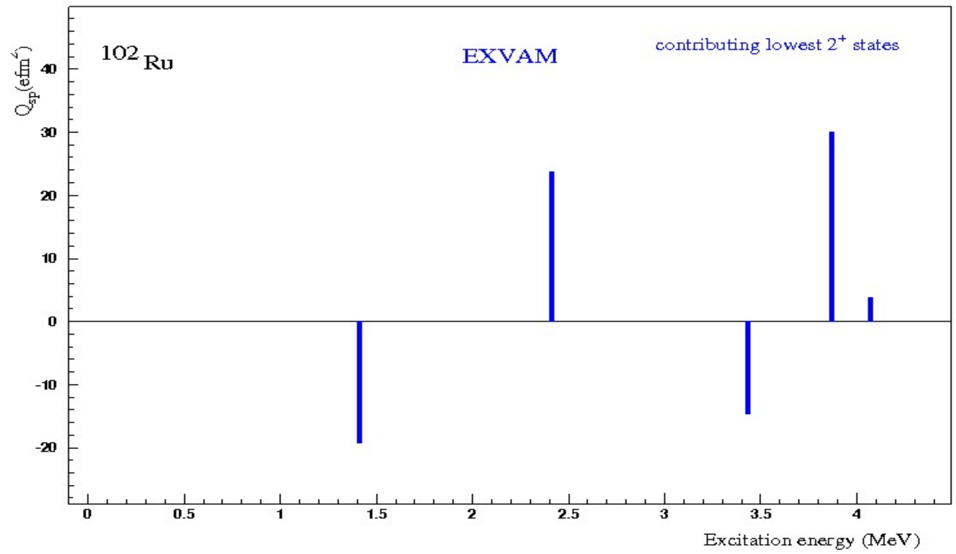

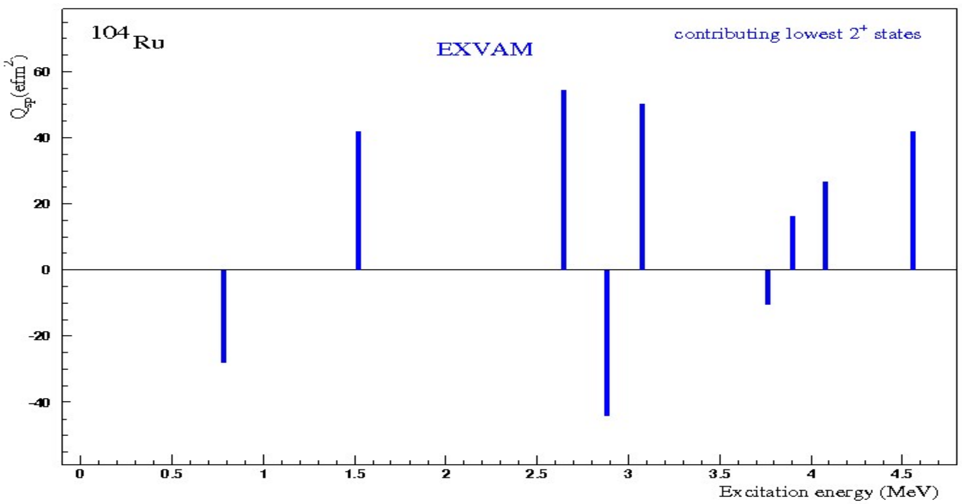

$^{104}Ru_{60}$

complex EXCITED VAMPIR bases:

25 orthogonal projected configurations

for the spins 2^+, 3^+, 4^+

Gamow-Teller contributing states

2^+ : from 82% to 9% prolate components

4^+ : from 96% to 8% prolate components

Spectroscopic quadrupole moments:

larger deformation for the N=60 states with respect to the N=58 ones

$^{102}Tc_{59} \rightarrow {}^{102}Ru_{58}$

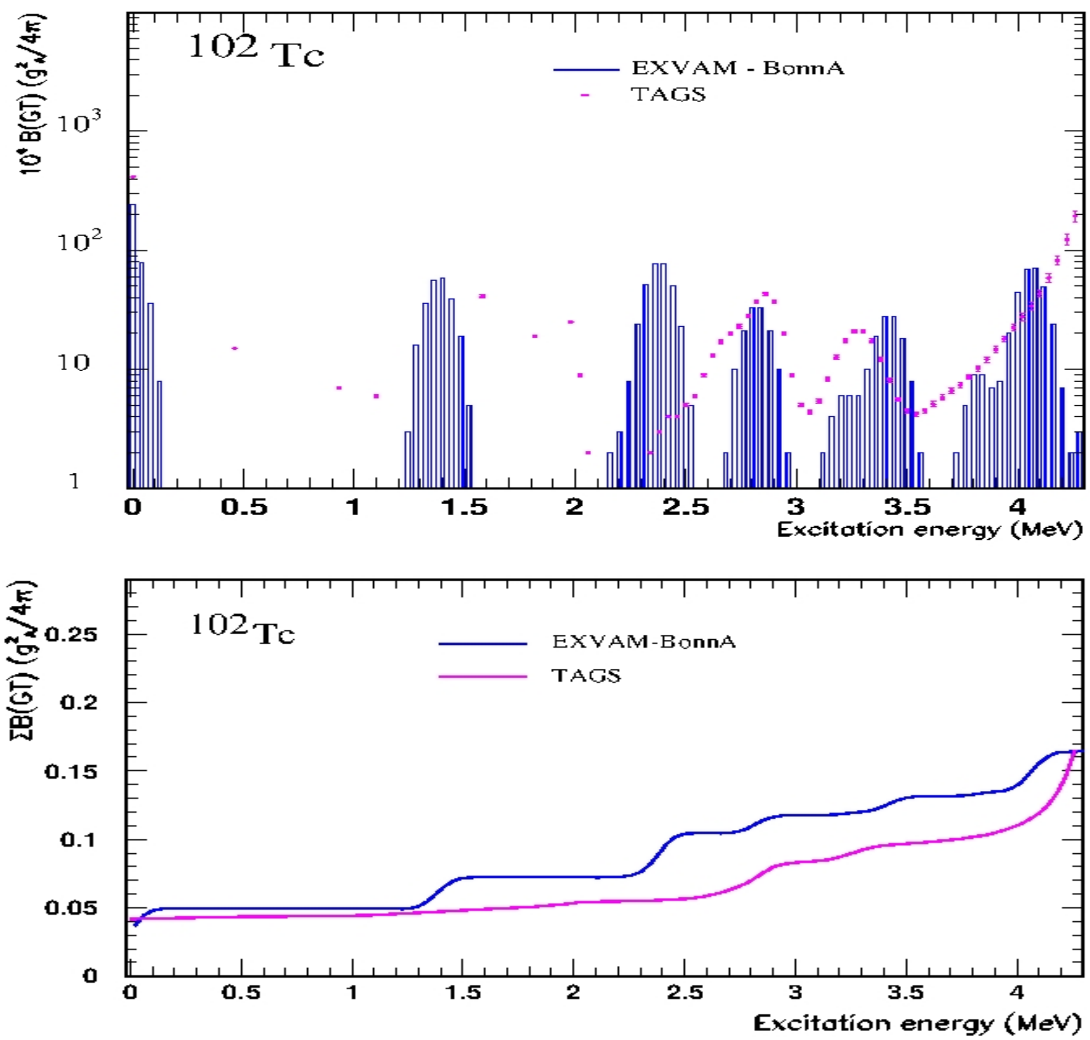

$T^{exp}_{1/2} = 5.3\ s$

$T^{EXVAM}_{1/2} = 6.6\ s$

Essential contribution from $g^{\pi}_{9/2} g^{\nu}_{7/2}$, $d^{\pi}_{5/2} d^{\nu}_{3/2}$, and $d^{\pi}_{5/2} d^{\nu}_{5/2}$ matrix elements

$^{104}Tc_{61} \rightarrow {}^{104}Ru_{60}$

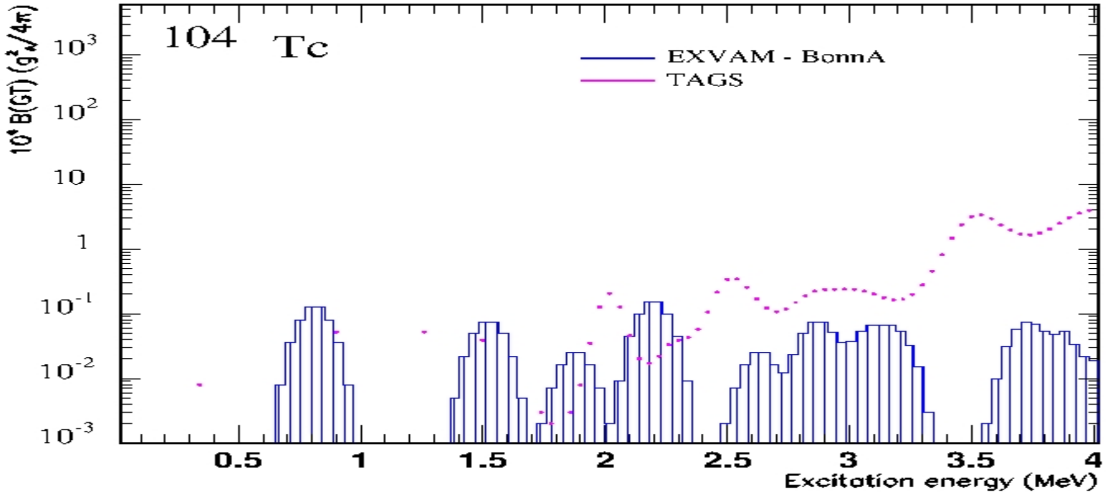

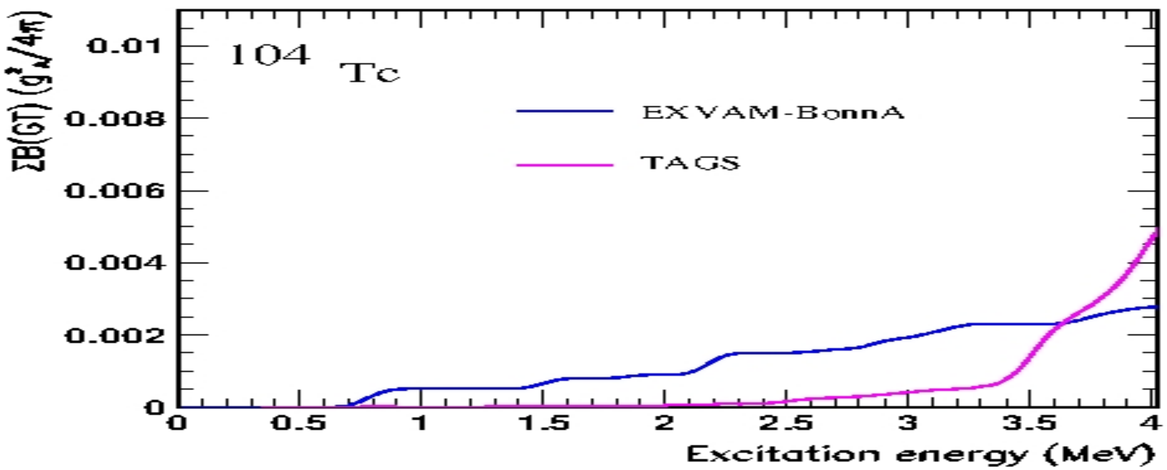

$T^{exp}_{1/2}$ = 1098 s

$T^{EXVAM}_{1/2}$ = 385 s

Contributions from $g^{\pi}_{9/2} g^{\nu}_{7/2}$, $d^{\pi}_{5/2} d^{\nu}_{3/2}$, $d^{\pi}_{5/2} d^{\nu}_{5/2}$, $p^{\pi}_{1/2} p^{\nu}_{3/2}$, $p^{\pi}_{3/2} p^{\nu}_{1/2}$ *matrix elements, all small, manifesting also cancellation effect*

Gamow-Teller β-decay half-lives and β-delayed neutron emission probabilities of Zr isotopes relevant for the r-process *A = 104, 106*

$^{98-110}$Zr chain : rapid transition → from spherical to deformed shape
shape coexistence → competing prolate, oblate, and spherical shapes

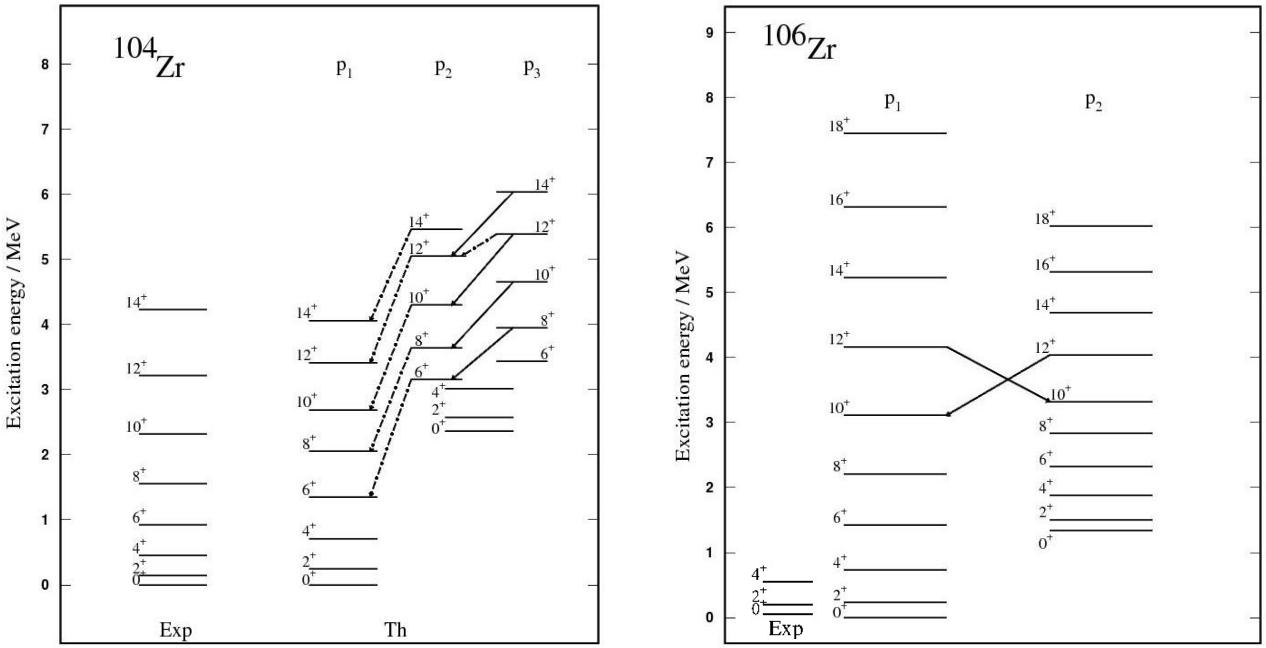

- *variable mixing of prolate deformed EXVAM configurations at intermediate and high spins*
- *ground state dominated (99%) by a strongly deformed EXVAM configuration*

A. Petrovici et al., J. Phys. 312 (2011) 092051

$^{104}Zr \rightarrow {}^{104}Nb$ $^{106}Zr \rightarrow {}^{106}Nb$ *NCSL-MSU / J. Pereira et al., Phys. Rev. C79 (2009) 035801*

A. Petrovici et al., Prog. Part. Nucl. Phys. 66 (2011) 287

complex* Excited Vampir many-nucleon basis: *50 projected 1^+ configurations in ^{104}Nb and ^{106}Nb

Gamow-Teller contributing states: large variety of spectroscopic quadrupole moments above 2 MeV excitation energy

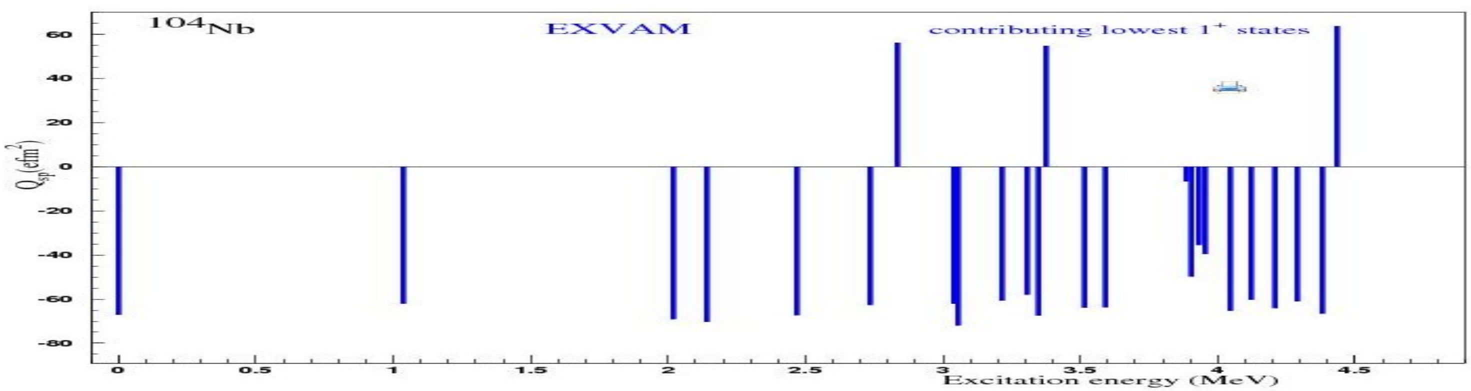

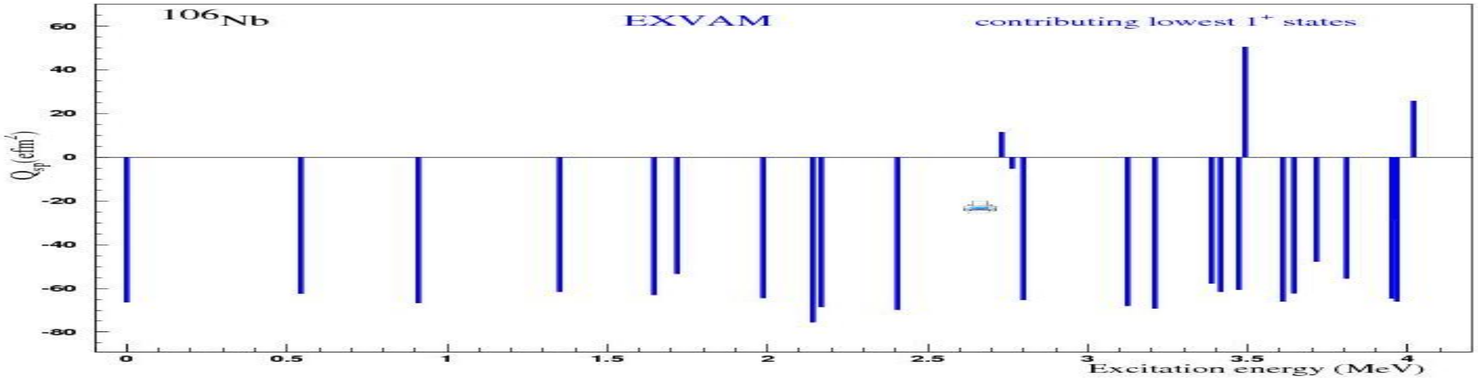

Gamow-Teller strength distribution specific for each isotope

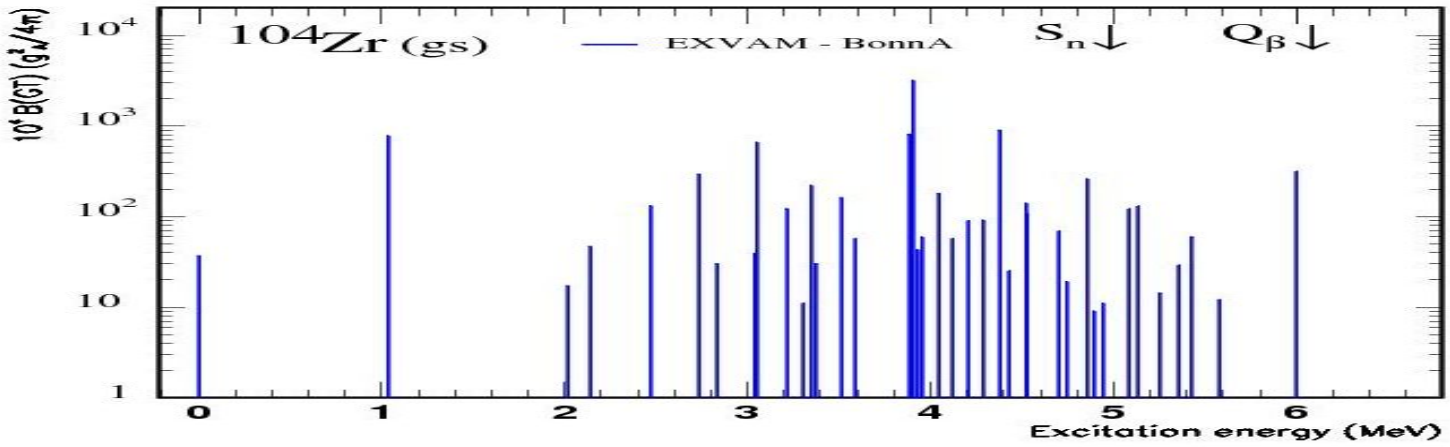

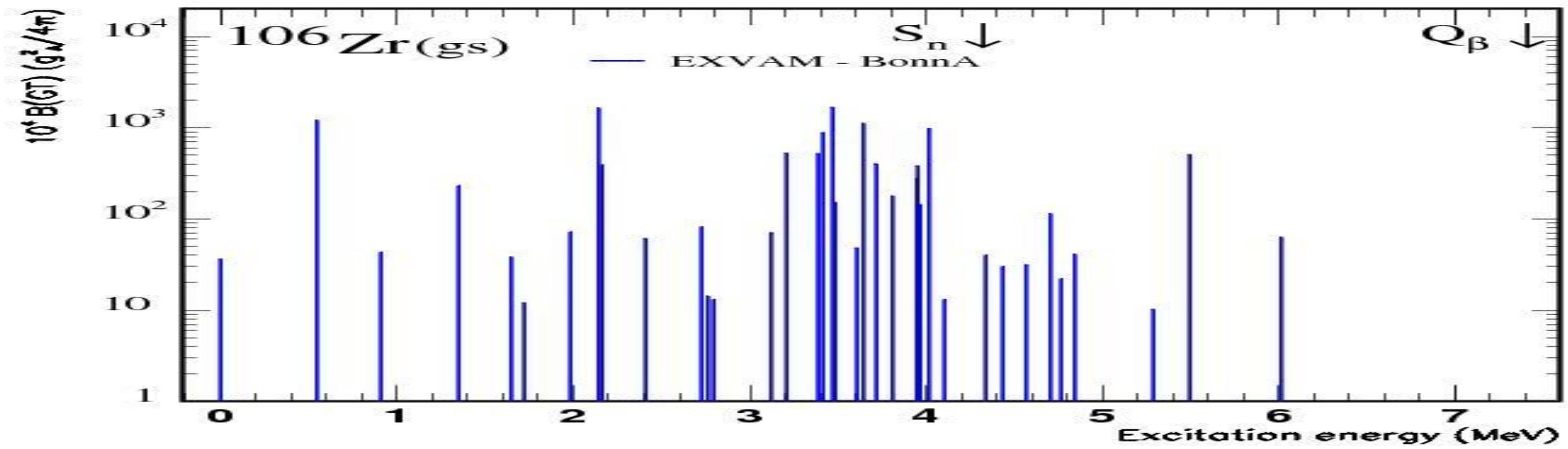

Essential contribution from $g^{\pi}_{9/2} g^{\nu}_{7/2}$, $d^{\pi}_{5/2} d^{\nu}_{3/2}$, and $d^{\pi}_{5/2} d^{\nu}_{5/2}$ GT matrix elements

Gamow-Teller accumulated strengths, half-lives, β-delayed ν-emission probabilities

$$P_n = \frac{\sum_{S_n}^{Q_\beta} f(Z, Q_\beta - E_{ex}) B(GT, E_{ex})}{\sum_{0}^{Q_\beta} f(Z, Q_\beta - E_{ex}) B(GT, E_{ex})}$$

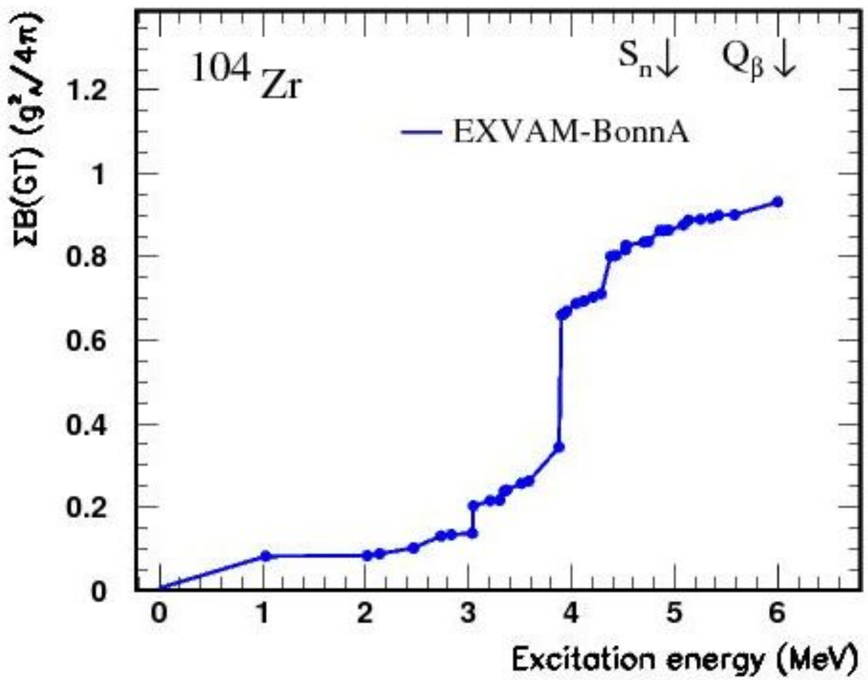

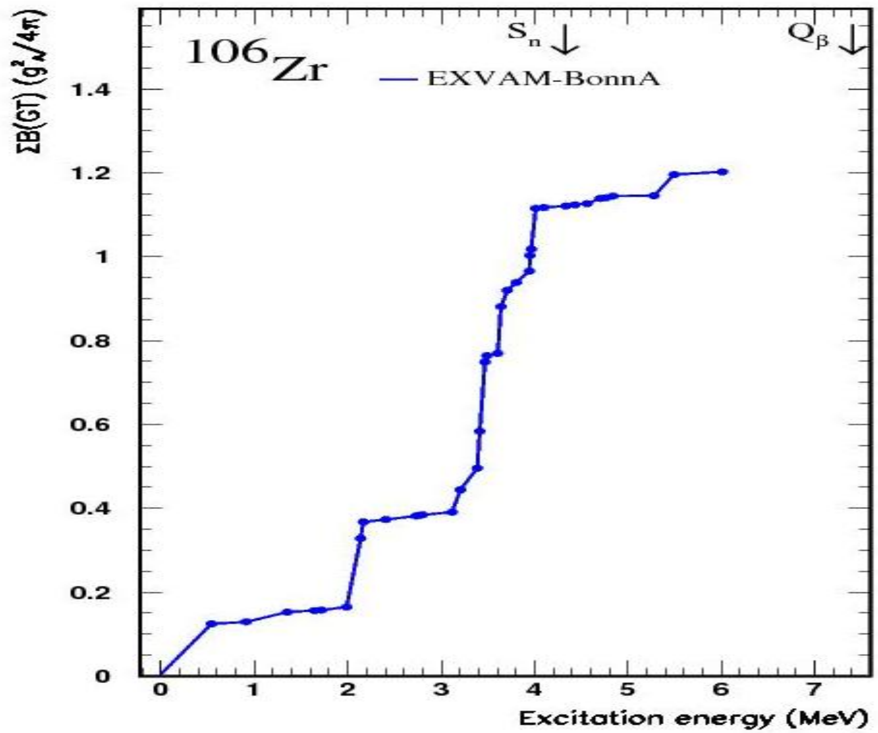

$T^{exp}_{1/2}$ 870(50)
(30) ms (MSU 2009)

P^{exp}_n < 1 % (MSU 2009)

1200(300) ms (Mainz 1980)

$T^{EXVAM}_{1/2}$ = 2040 ms
(50 1^+ states in ^{104}Nb)

P^{EXVAM}_n ~ 1 ‰

$T^{exp}_{1/2}$ 260(20)
(30) ms (MSU 2009)

P^{exp}_n < 7 % (MSU 2009)

$T^{EXVAM}_{1/2}$ = 230 ms
(50 1+ states in ^{106}Nb)

P^{EXVAM}_n ~ 2 %

Summary and outlook

complex **EXCITED VAMPIR model explains self-consistently**

- **experimental trends in the N=58 Sr and Zr isotopes manifesting shape coexistence and mixing :**
  - triple coexistence of spherical, prolate, and oblate configurations in the structure of lowest 4 0^+ states
  - multifaceted yrast structure specific for ^{96}Sr and ^{98}Zr

- **large prolate deformation in ^{104}Zr and ^{106}Zr**

- **Gamow-Teller *β*-decay and *β*-delayed neutron-emission for $^{104,106}Zr$**

- **remarkable difference in the Gamow-Teller *β*-decay of ^{102}Tc and ^{104}Tc revealed by TAGS data**

The effective interaction for the A~100 region is currently improved starting from a G-matrix based on Bonn CD potential